J Pharm Innov (2017) 12:26–40
DOI 10.1007/s12247-016-9266-5

ORIGINAL ARTICLE

Process Understanding in Freeze-Drying Cycle Development: Applications for Through-Vial Impedance Spectroscopy (TVIS) in Mini-pilot Studies

Geoff Smith[1] · **Muhammad Sohail Arshad**[1,2] · **Eugene Polygalov**[1] · **Irina Ermolina**[1] · **Timothy R McCoy**[3] · **Paul Matejtschuk**[4]

Published online: 26 November 2016

Abstract
Purpose The freeze-drying cycle comprises three stages: (1) freezing, to form ice and to crystallise out any solutes with a propensity to crystallise, (2) primary drying to remove the ice phase by sublimation and (3) secondary drying to remove the remaining unfrozen water which is bound to the remaining matrix of crystalline and amorphous solids. Given the impact of scale on the process outcomes, any freeze-drying cycle developed based on mini-pilot studies will inevitably require measurement technologies for characterising each stage of the cycle at each scale of the process. However, there are inherent challenges in the development of reliable mini-piloting studies, with the first being the fact that no single PAT technology for freeze drying may be implemented across all levels of scale, and the second being the inherent changes in process characteristics (process parameters that result from scale-up).
Methods Here, we present a new approach for process understanding in freeze-drying cycle development, which uses a through-vial impedance measurement.
Results The technique has been used to characterise a broad range of features of the process, including, ice onset times, the completion of ice solidification, the glass transition and the structural relaxation of the amorphous solid, a surrogate for primary drying rate and the primary drying end point.
Conclusions The on-going development of this technology may see the application with microtitre plate technologies for formulation screening (microscale down) and for scale-up into production by using a non-contact probes for monitoring problematic regions within the dryer.

Keywords Freeze drying · In-line process control · PAT · QbD · Critical process parameters

Introduction

The scale-up of a lyophilisation cycle is challenging due to multiple differences between small- and large-scale dryers. There is some guidance to facilitate the development of an efficient lyophilisation cycle in the laboratory (1); however, even an optimised cycle from a laboratory freeze dryer may not transfer smoothly to the manufacturing scale. In addition to the scalability differences, there are several other differences between laboratory and manufacturing scale lyophilisers, which may pose a serious challenge for scale-up. These challenges include the following: (i) ice-nucleation differences during freezing, (ii) heat and mass transfer differences and (iii) differences in primary drying time. These differences between laboratory and manufacturing scale lyophilisers can pose a serious challenge, and therefore, a systematic approach is needed to ensure a smooth scale-up.

There are a number of stages in a typical lyophilisation process: freezing (sometimes including annealing) which transforms the liquid solution into a stable frozen matrix, primary drying to remove the ice and secondary drying to remove residual water from the unfrozen super-cooled liquid domains of the material [1]. Whilst on the surface these stages

✉ Geoff Smith
gsmith02@dmu.ac.uk

[1] Pharmaceutical Technologies Group, Leicester School of Pharmacy, De Montfort University, Leicester LE1 9BH, UK

[2] Department of Pharmacy, Bahauddin Zakariya University, Multan, Pakistan

[3] Genzyme (a Sanofi Company), IDA Business Park, Old Kilmeaden Road, Waterford, Ireland

[4] National Institute for Biological Standards and Control (NIBSC), South Mimms, Potters Bar, Herts EN6 3QG, UK

appear to be somewhat discrete, they in fact constitute a sequential series of inter-dependent events. The process kinetics (ice formation, sublimation and moisture desorption) are driven by a number of factors, including heat transfer through the vial base and walls (impacted by any thermal heterogeneities in the shelf temperature and radiant heating on the edge vials), the structure of frozen matrix which evolves from the stochastic ice formation process and the initial water content of the interstitial spaces [2]. Any attempt to investigate the freeze-drying process is complicated by the fact that the process is undertaken in a closed system, under extremes of temperature and pressure settings, within a batch of vials in close proximity to each other and many (>10,000) in number, meaning that direct access by any PAT sensors is limited.

It is also widely recognised that any attempt to predict product-scale process parameters from the laboratory scale is complicated by the fact that the scale of the operation has a significant impact on the process outcomes. There will be variations in the process parameters, and hence the dependent critical quality attributes, that are considered to be a function of the process scale and care should be exercised to avoid developing a cycle at the mini-pilot scale that cannot be translated to the large-scale production [3].

It is nevertheless the intention within a scale-down/scale-up approach to use intermediate or benchtop-scale studies to gain product and process knowledge that helps predict the behaviour (scale-up), assess risks (risk analysis) and diagnose production issues (troubleshooting) at production scales. There will inevitably be limitations to what can be achieved, but so long as various factors are considered in the design of a meaningful mini-pilot study then one may be able to maximise the relevance of mini-pilot data to the larger-scale production process [4]. The factors to be considered have been discussed elsewhere [5] but include the following:

1. Formulation composition—for instance, incomplete crystallisation of excipients such as mannitol or glycine [6] with consequential heterogeneity in moisture, crystallinity and appearance.
2. The freezing step—as it defines the ice crystal size, which then defines the pore size for sublimation to occur [7]. Variations in freezing rates associated with differences in temperature at locations around the dryer, coupled to the stochastic nature of super-cooling and nucleation, inevitably introduce heterogeneity [8]. Controlled nucleation is showing promise in delivering shorter primary drying times and greater product homogeneity [9]. Mini-piloting studies might therefore aim to simulate the controlled nucleation that is sometimes practised at the larger scale in an attempt to understand the fast kinetics of the process. However, that may require the development and implementation of new forms of measurement system to track those bulk nucleation and growth phases which result in less-efficient secondary drying due to lower surface area.
3. Cycle design and system capabilities—where a cycle is designed at laboratory or pilot level, the process conditions applied cannot always be achieved in the same way within an industrial scale unit, owing to a number of factors: (i) the rate at which vacuum can be applied may be different between a laboratory system and a production model, especially where process routines require oil free (Rootes) pumps; (ii) the nature of the valve between the chamber and the condenser can also differ between small units (where indeed for some lab models the condenser is inside the chamber) and production units; (iii) the design of the valve and its speed of response, as well as length and diameter of vapour duct, must be taken into account as potential sources of variation on scale-up and indeed may make pressure rise testing impractical; (iv) cooling/heating rates of a mini-pilot dryer and a large process-scale machine may differ significantly with the latter only being able to achieve low rates of temperature change owing to the thermal inertia of a large dryer; (v) there may be a significant difference between the temperature achieved on one shelf and another of a large stack of shelves or the time taken to achieve a given temperature across a large stack may differ from the one observed for a small single shelf mini-pilot unit; and (vi) the smoothness or 'roughness' of the finish on the shelves and the flatness of the shelves are factors which must be considered as the creation of a space between the shelf and the base of the vial will influence heat transfer from the shelf to the product. These factors would be difficult if not impossible to model at small scale. Instead, the freeze-drying cycle for a production scale dryer may require adjustment in the shelf temperature and chamber pressure in order to achieve the target product temperature.
4. Impact of scale on sublimation rate—the design of a freeze-drying cycle for process scale, if based strictly on a mini-pilot data may be too ambitious for the reasons above. Calculation of the heat transfer properties of the freeze-drying system, thermal coefficient of the vial, resistance to vapour flow posed by dry cake and the gradient in pressure between sublimation front and condenser allow greater predictability to the scale-up (1, 2, 7 and 8). In primary drying, it is essential that the product temperature is maintained as high as possible in order to maximise sublimative cooling and reduce the primary drying time, whilst maintaining the product temperature below certain critical temperatures (the eutectic temperature (crystalline) or glass transition (partially or fully amorphous) in order to avoid melt-back or collapse. Engineering factors to consider in process optimisation and scale-up include the following: (i) minimum achievable pressure as a function of sublimation conditions; (ii)

maximum sublimation rates before losing control of pressure or choke flow; (iii) condenser temperature; as the driving force for sublimation is the pressure gradient due to the pressure at sublimation surface of the product and the pressure at the surface of the ice on the condenser coil; (iv) the vial heat transfer coefficient-conduction (heat vial contact between the vial base and the shelf); (v) convection (heat transfer through gas phase); (iii) radiation (heat transfer from walls, underside of the upper shelves etc.); and (vi) the amount of radiant heat entering through the transparent Perspex door of the freeze dryer, the scale of the shelves and the heat radiated from the walls are all likely to be very different between a mini-pilot dryer and a process dryer, whilst formulation, vial and stopper format remain constant. The impact of shelf, the effect of nearest-neighbour interactions and the impact of radiant heat from the shelves above (and hence the inter-shelf distance) are all factors to bear in mind on scale-up [10]. The mapping of sublimation heterogeneity across a shelf has been well demonstrated, with the centre of a tray of vials and indeed the centre tray of a series of vials on a shelf, drying more slowly than those at the extremities where external heating effects are greater. Radiation is the dominant mode of heat transfer during lyophilisation [11], and the edge vials experience most radiation, hence the increased product temperature and therefore rate of sublimation for the edge vs centre vials.

Process Monitoring and Process Analytical Technology It is clear that the prudent use of process analytical technology (PAT) is a key factor in being able to achieve an effective scalable freeze-drying cycle. There are many different technologies for monitoring and even controlling the freeze-drying process, and these have been reviewed elsewhere in a number of comprehensive texts [3, 12–17]. However, these technologies have not been reviewed within the concept of mini-piloting which includes the use of emerging physical characterisation techniques that could significantly improve the measurement of process parameters and product-quality attributes during drug development and manufacturing that would potentially replace or supplement traditional approaches in the near future.

The inevitable question therefore is "which technologies could be used for mini-piloting studies?" Before addressing that question it is worth stating that mini-piloting studies in freeze-drying may take on a number of forms, in terms of the scale length being investigated. Here we define a number of sample and batch scales which could be considered for the concept of a mini-piloting study: (1) mini-vials and microtitre plates (<1 ml)[1] in which the size of the sample and container is reduced from that expected of the final product; (2) single vials (2–50 ml)[2] to be used for a fill volume to be used for the final product; or (3) clusters of these vials (modelling the impact of radiant heat from the walls of the dryer) where the total volume for each study is defined by the number of vials in the cluster multiplied by the fill volume.

Mini-vials and microtitre plates have been used to effect for high-throughput formulation screening [18–22]. However, due to the fact that the change in sample size in relation to container geometry (wall and base thickness and materials of construction) has a significant impact on the freezing and drying processes, which is currently difficult to model, then such systems may not be considered presently for a mini-pilot application. Moreover, the commercial sample scale is determined by the product requirements and is not therefore considered as a variable in the development process: once the formulation has been selected (with or without the use of a high throughout methodology), the process is developed based on a predefined container size and fill volume (and hence fill height). Mini-pilot studies can therefore be considered from a starting point of a single vial.

Here, we make a definition of cluster size in terms of micro cluster and meso cluster in order in order to recognise the fact that edge effects extend over the outer three to four rows of vials in a large cluster, which means that all vials in a microcluster will dry as edge vials, whereas a mesocluster will have some edge vials and some core vials. It is invariably the case that, for the early-stage process development, where there is a requirement to minimise the solution volume (and hence drug consumed), the impact of edge effects is removed by placing the product containing vials at the centre of an array of empty vials.

Having clarified the definitions and the impact of scale length in terms of numbers of vials, one then can delineate which PAT might be useable for each scale. Table 1 lists a number of commercial PATs and research tools that have been defined as being suitable for each of these scale lengths, whereas others have been excluded. As stated above, it could be argued that microplates and mini-vials are best suited for initial formulation screening [18], and their use in predicting scale-up is quite limited. These systems are therefore excluded from the scope of a mini-pilot study. Given that mini-piloting must start form a single vial, then one might expect that the model single vial systems that have been described and the seven vial model lyophiliser might be useful in this regard [23]. However, the use of such systems for a mini-pilot study should be used with caution owing to the fact that a single vial (or a microcluster of seven vials) will behave very differently to a vial in the centre of a meso- or a macrocluster. The impact of radiant heating on the drying characteristics (shape of the drying front and product temperature) are significantly different for a lone vial to a vial within a large cluster.

[1] These are not used in production of any commercial product.

[2] These are the vials that are currently available for most commercial products.

Table 1 Comparison of analytical technologies for assessment of critical quality attributes and process parameters

Sample presentation	Stage	Potential PATs	Excluded PATs
Microtitre plate	Formulation screening	Uv-vis, Raman, fluorescence and TC	Pressure rise and TDLAS
Single vial	Mini-pilot scale to pilot scale	OCT, TVIS, NIR, Raman, RTD, TC and microbalance	Pressure rise and TDLAS
Microcluster (7, 19 and 37 vials)	Mini-pilot scale to pilot scale	• TC, RTD, TVIS and smart sensor • NIR and microbalance ("edge" vial only)	Pressure rise and TDLAS
Mesocluster (61, 91, 127 and 169+ vials)	Pilot scale	• TC, RTD and TVIS • TDLAS and pressure rise (demand a minimum number of vials) • NIR and microbalance ("edge" vial only)	
Macrocluster (10,000+ vials)	Production	TC, pressure rise and TDLAS	Microbalance

The table includes both commercially available systems and those which are currently available only in specific research laboratories

NIR near infrared, *TC* thermocouple (ideally wireless), *TVIS* through-vial impedance spectroscopy, *OCT* optical computer tomography, *RTD* resistance temperature detector

It is clear that each PAT technology is somewhat limited in its application across all scales within the development cycle, and it remains the case that there is no single PAT technology that can be applied to assess all quality attributes of the product and process parameters of the cycle, at all levels of scale. There are a number of reasons for that, with each pertaining to the PAT in question and the target process parameter for that particular technology. Two process parameters (critical temperatures and drying rates) and one material attribute (glass formation) are used to illustrate this point.

Critical Temperatures Single vial systems have been developed for the purpose of evaluating other more novel process analytics, e.g. optical coherence tomography (OCT) measurements of collapse [19]. These are beneficial as they demonstrate a minimum requirement that the analysis of some process parameter or material attribute should be conducted, at least within a container and sample volume that is consistent with that being freeze dried at the larger scale. This implies that techniques such as conventional freeze-drying microscopy (FDM) may not accurately define the critical parameters (temperatures required to control the process), however they are used extremely frequently and widely in the formulation characterisation process [24].

In attempting to drive process efficiencies, one tries to maintain the product temperature as high as possible in order to supply the latent heat of sublimation. However, this is complicated by the following issues: the product temperature is always lower than the shelf temperature owing to the heat absorbed from the sublimation of ice and the fact that it is difficult to measure the temperature at the sublimation interface. TCs placed in the base of the vial can be used to assess the end point of primary drying (for example), but their position at that point precludes the assessment of the temperature at the sublimation interface, which inevitably moves down the vial contents as the drying process progresses. A technique that can measure the product temperature at the ice sublimation front will inevitably provide greater assurance that the temperature at the sublimation interface does not fall below the critical temperature at which the dry layer (in immediate contact with the sublimation interface) does in fact collapse. The implementation of such a PAT tool within the process control loop will inevitably reduce the risk of product failure through over-aggressive drying profiles. In addition, single vial TCs only provide information on thermal events (and the end point of drying) but not the drying rate.

Primary Drying Rates

Pressure rise and tunable diode laser absorption spectroscopy (TDLAS) techniques are used for the measurement of mass flux and drying rates within dryers that are either partially or fully loaded. However, the determination of drying rates as a function of the location of the vial within a cluster is not accessible with these technologies. A commercially available alternative, i.e. the microbalance, can work at the scale of a single vial but only works on an isolated vial or one which is on the edge of a cluster (which inevitably experiences greater radiant wall effects and does not simply rely on heat transfer through the base). Drying rates and dry-layer product resistance calculated by this technique therefore should be used with caution when applied to the behaviour of the same materials when freeze dried within clusters, owing to the significant impact from radiant heating of the side of the glass vial. It is also the case that single vial spectroscopies cannot be used on clusters of vials; any information on product quality (e.g. protein folding by Raman) and water content during drying cannot be easily translated to populations of vials (because the probes are large and will inevitably cause significant disruption to the thermal heat treatment experiences by vials embedded with a manufacturing scale cluster). It is also apparent that

existing PATs are limited in their ability to 'look inside' the vial with most optical spectroscopy being limited to a surface measurement of 1–2 mm at best. That said, the application of optical spectroscopy for single-vial measurements is the subject of renewed interest, given the potential application in the freeze drying of vials in a continuous process, where such technologies are expected to excel [25–27].

The Amorphous State (Mesoscopic Properties and Glass Formation)

PATs which enable the measurement of mesoscopic properties (i.e. the material properties at the scale length of molecular clusters) such as the glass transition and the fragility/strength of the glass are desired as these properties have significant impact on the product and process efficiency. The formation of the amorphous phase depends to a large degree on the amount of ice that in turn defines the water content of the unfrozen fraction. In addition, the rate at which the amorphous state forms and the temperatures at which the amorphous phase forms will inevitably influence the enthalpy entrapped within the interstitial phases. The power of molecular vibrational spectroscopies has been well-demonstrated [27]. These parameters impact the secondary drying phase [28] and even the stability of the glass matrix that forms [29].

Application of PAT Across the Scales

One key requirement might be that the prospective analytical technology in question has itself a potential for scale-up [30]. The principle drawback of mass-flow-based PAT techniques is that these display only one temperature value for the entire batch and do not take into account the inter-vial heterogeneities in different locations of the shelf, which are evidenced through individual temperature sensing devices. Generally, the product temperature values obtained from the manometric temperature measurement (MTM) technique (used for small scale) are believed to be related with the colder region of the shelf that is non-edge or centre of the array and that temperature as low as −45 °C during primary drying may be determined with this technique [31]. End point of primary drying is characterised by a sharp drop in vapour pressure of ice. MTM lead product temperature measurement has been fairly representative with first 2/3rd of the primary drying time; however, after this time, heterogeneities in the rates of ice sublimation amongst vials located at different position in the shelf are predominant [32]. Therefore, the PAT measured product temperature after this point of time may be non-representative of the actual product temperature [12, 32]. Furthermore, the heat transfer rates were misleading when lyophilisation cycles were performed at very low temperatures and low pressure [33] using low solid contents [31] whilst a minimum sublimation area of 150 cm^2 is required for an accurate MTM product temperature measurement. Lyophilisation of the formulations with high amorphous solid contents were measured inaccurately with MTM, especially in the early phase of primary drying resulting in a high drying temperatures due to re-adsorption of vapours in the dried layer due to pressure rise [12, 34]. Lastly, the closure of MTM valve hinders the sublimation process owing to slowed self-cooling which may sequence to collapse if the freeze-drying cycle is operated at temperatures close enough to collapse temperature [12] or if extended isolator valve closure periods are used.

TDLAS, another PAT measures the rate of sublimation from the whole batch by recording the light absorption during the passage of vapour through the duct connecting the drying chamber and the condenser [35, 36] provided that the freeze drier requires having a conducting duct of an appropriate length. This can be used in process to feedback and control the freeze-drying cycle as in the LyoStar (Virtis) range of dryers.

Both MTM and TDLAS have been used to develop a series of models for the freeze-drying process and also to build those algorithms into the first smart freeze-drying processes that allow control on-line to be achieved either by intervention or automatically [37]. However, the application of these tools in mini-piloting of freeze-drying process is somewhat limited given the requirement for a minimum batch size.

As stated above, mini-pilot data may not translate appropriately through scale-up unless the PAT technology used to assess the process is also transferrable between scales, and thereby provide an opportunity to unify the PAT signatures at each scale length. For example, in the case of protein formulations (which are sensitive to freeze-concentration stresses) then mini-pilot data from a single vial or microcluster of vials may not translate to larger clusters within bigger dryers because the way the sample freezes could impact factors such as aggregation of the active.

Techniques which might bridge the gap between the small scale (e.g. single vial freeze dryer to the production scale) are limited. One of the few examples are wireless temperature sensors [38] which are an improvement over classical thermocouple or resistance thermometers owing to the lack of wiring, and compatibility with automated loading systems but they are still very much tools used in development, invasive in nature and perturb the ice formation as well as sublimation kinetics. There is an unmet need for a non-invasive technique that can measure both critical events, such as ice formation, glass transition and solidification and collapse, whilst being able to measure drying rates and end points, and to able to do that across a range of scales from the single vial to multiple vials within clusters, so that the impact of both vial base and radiant wall heating can understood in terms of its impact on process parameters and critical quality attributes. In essence, it is essential that both core and edge vials are assessed for

conformity with specification so that the mini-pilot data can be assessed in terms of its direct relevance to production scale and that risks to product quality are understood and mitigated. A more recent PAT technology based on through-vial impedance spectroscopy (TVIS) has been introduced to partly fulfil this need. This technology is non-contacting to the product (unlike an invasive impedance probe in a vial (such as CHRIST's LyoControl technology [39]) and provides some opportunity to characterise material properties across the scales. Albeit in its current form it is a single vial measurement, the opportunity exists to use multiple sensors to track different regions of the dryer and at different scale lengths; and in the future, the potential development of a non-contact format may allow for such measurements in both scale-down application (within mini-vials or microwells) and for scale-up for multi-vial clusters. The latter is currently the subject of a UK government-funded Innovate UK project called Biostart. Theoretical feasibility has been established and a demonstrator unit is currently under development.

Through-Vial Impedance Spectroscopy

Impedance monitoring has a long history as a lyophilisation analysis tool [40, 41]. TVIS measures the electrical impedance of the product, contained within a standard freeze-drying vial that has been modified with electrodes placed on the outside of the glass wall [42]. The impedance measurement vial is connected to a low input-impedance, current to voltage convertor (IVC), via a junction box within the freeze-dryer chamber (mounted close to the shelf on which the vials are located). The signals from the stimulating voltage and that from the resultant current (from the I-to-V convertor) [43] are compared in order to determine the impedance of the measurement vial (and its contents) (Fig. 1). The calibration of through-vial impedance measurement system is performed by taking in account the impedance contribution at open loop as well as close loop conditions using a reference standard of known capacitance. Details are described in the literature [42].

The technology combines the function of different single vial PATs (viz. thermocouple and microbalances) but with a number of advantages: the measurement electrodes are non-intrusive to the product volume or head space (unlike a thermocouple) which means that the system will not interfere with the processes of ice nucleation and growth. The measurement hardware has minimal thermal mass and volume (unlike the microbalance). This minimises the impact on heat transfer whilst facilitating measurements on vials which are arranged in the usual hexagonal array (a requirement for maximising the number of vials loaded into the freeze dryer). Although the present design of impedance measurement vials does not support automatic loading, the use of thin foil electrode makes the tests vials suitable for their placement at any position within the hexagonal array. This feature, in turn, suggests the potential application of TVIS in spatial mapping of the shelf. A multichannel (TVIS) instrument design enables the placement of impedance measurement vials at different positions across

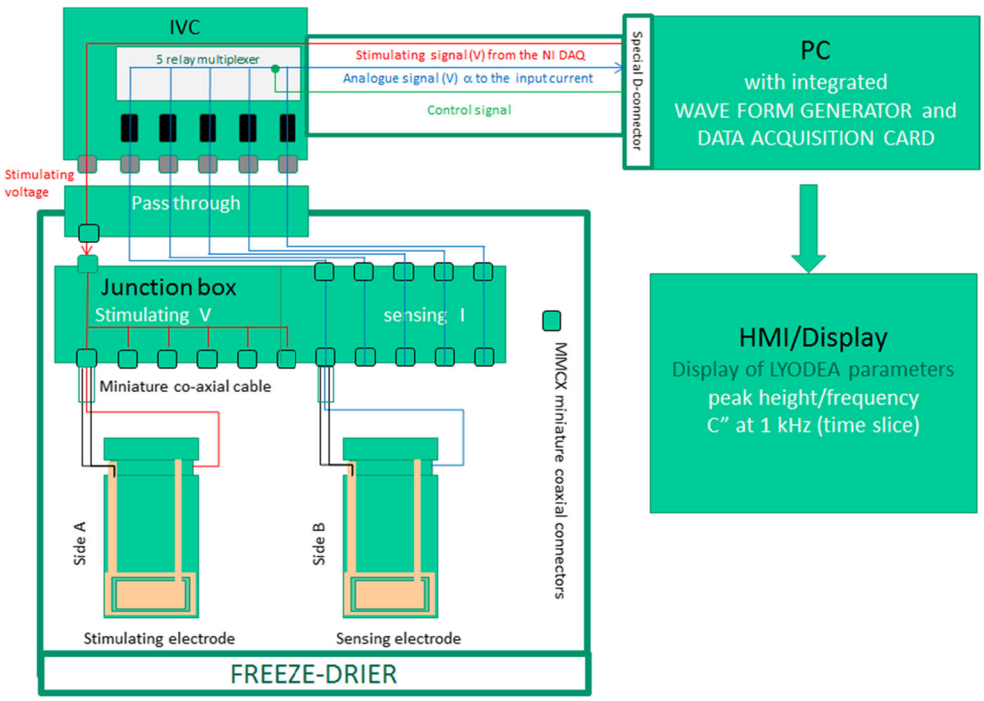

Fig. 1 Block diagram of the impedance measurement system. Sides A and B are part of the same vial

the shelf which can map the shelf for temperature distributions and variations in the drying rates and to guard against the potential for product collapse.

Electrical Impedance

The electrical impedance of a material determines how easily the material will conduct a current when an alternating voltage is applied to it. Electrical impedance is a function of both the dielectric and conductive properties of the material which are in turn defined by the temperature, composition and physical state of the material contained within the vial (an example TVIS vial is shown in Fig. 2 (i)). Changes in these electrical parameters therefore directly mirror the condition of the sample and the progression of the freeze-drying cycle. In order to explain the observed impedance spectrum of the object under test and relate it to the physical properties or changes that may happen during the freeze-drying process, it is necessary to create an appropriate equivalent circuit model. The circuit model (Fig. 2 (ii)) was found to provide an approximate fit to the measured impedance spectrum, where C_G signifies the electrical capacitance of the glass walls of a vial, which is charged through the resistance (R_S) representing the conductivity of the sample, and C_S represents the electrical capacitance of the material within the internal volume of a vial. This imparts a frequency-dependence to the measured dielectric properties, such that the capacitance of the glass wall (C_G) will have sufficient time to charge completely at low frequency, but at high frequency, will not have time to begin to accumulate any of the electrical charge that could otherwise be accommodated.

The overall result is that the capacitance spectrum of the material under test (i.e. glass vial, its contents and the electrical connections to the vial) will display a step-like decrease in capacitance as the frequency is increased through that critical frequency which corresponds to the time constant for the sample ($f = 1/2\pi\tau$, where $\tau = R_S(C_G + C_S)$) (Fig 2 (iii, top)). There is a corresponding peak in the associated imaginary capacitance spectrum as the material under test starts to conduct electricity through the phase lag between the response of the sample and the applied electric field (Fig. 2 (iii, bottom). The step in the real-part capacitance and the peak in the imaginary capacitance are the manifestations of what is known as an interfacial-relaxation process. It is a consequence of the time dependence of the accumulation of charge at the glass surface as ions migrate through the liquid (or solid) contained within the glass vial, following the application of an external field [44].

It is the characteristics of this process that are used to 'follow' the progression of the freeze-drying cycle. More specifically, it is the peak frequency and peak value for the imaginary capacitance (which can be considered as the magnitude of the interfacial-relaxation process) that is used to monitor the freeze-drying cycle. Figure 2 (iv) shows a typical surface plot of the imaginary capacitance as a function of frequency and time, during the entire freeze-drying cycle. There are characteristic shifts in the relaxation frequency and change in the peak height as the temperature of the sample changes and when the material undergoes a phase change (e.g. liquid to

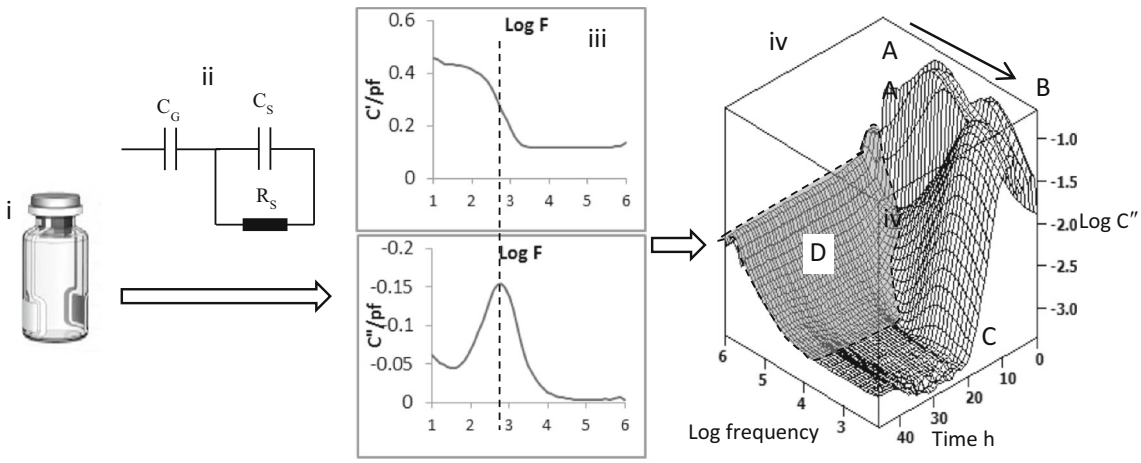

Fig. 2 Description of measurement principles; from *left* to *right*, *i* TVIS measurement vial with external electrodes attached (in this particular variant, there are guard electrodes around each of the measurement electrodes), *ii* equivalent electrical circuit, with C_G modelling the capacitance of the glass wall of the vial, and C_S and R_S modelling the capacitance and resistance of the contents of the vial, *iii* individual spectrum (C' vs log frequency is the real-part spectrum, C'' vs log F is the imaginary part spectrum) where the frequency of the peak in the imaginary capacitance is given by $f = 1/2\pi R_S(C_G + C_S)$ (Note that this particular spectrum is taken after freezing the sample), and *iv* response surface plot of imaginary capacitance, resulting from measurements at a range of temperatures. The peak at position A in the early stages of the cycle shows the condition of the sample in the liquid state. The peak shifts to position B (lower frequencies) when the sample freezes and the product resistance increases by a factor of 100–1000. The decrease in the peak height over time is a consequence of the loss of ice on sublimation during the primary drying phase. The wing at low frequency (*shaded area D delineated by the dotted line*) is more than likely to be due to the additional distributed element characteristics of the glass wall

ice) [45]. There is then a dramatic decrease in the magnitude of the interfacial-relaxation peak as ice is removed from the sample. Factors such as salt content, buffers and tissue culture medium will increase the conductivity and shift the relaxation peak to the higher frequency end of the experimental frequency window.

The impedance of the object under test (namely the glass vial and its contents) can be calculated from the following equation

$$Z^* = \frac{1}{i\omega C^*} = \frac{1}{i\omega C_G} + \frac{1}{\frac{1}{R_S} + i\omega C_S} \tag{1}$$

From the complex impedance formula, the expressions for real and imaginary capacitance can be calculated to explain the origin of interfacial polarisation peak

$$Z^* = \frac{1}{i\omega C_G} + \frac{R}{1 + i\omega R_S C_S} = \frac{1 + i\omega R(C_S + C_G)}{i\omega C_G - \omega^2 R_S C_S C_G} \tag{2}$$

$$C^* = \frac{1}{i\omega Z^*} = \frac{C_G + i\omega R_S C_S C_G}{1 + i\omega R_S (C_S + C_G)} \tag{3}$$

By multiplying nominator and denominator by the complex conjugate of denominator

$$C^* = \frac{1}{i\omega Z^*} = \frac{(C_G + i\omega R_S C_S C_G)(1 - i\omega R_S (C_S + C_G))}{(1 + i\omega R_S (C_S + C_G))(1 - i\omega R_S (C_S + C_G))} \tag{4}$$

$$= \frac{C_2 + \omega^2 R_S^2 C_S C_G (C_S + C_G) - i\omega R_S C_G^2}{1 + \left(\omega R_S ((C_S + C_G)\right)^2} \tag{5}$$

and grouping the real and imaginary members decomposes C* into its real C′ and imaginary parts

$$C' = \frac{C_G + \omega^2 R_S^2 C_S C_G (C_S + C_G)}{1 + \left(\omega R_S ((C_S + C_G)\right)^2} \tag{6}$$

and

$$C'' = -\frac{\omega R_S C_G^2}{1 + \left(\omega R_S ((C_S + C_G)\right)^2} \tag{7}$$

For an example spectrum (Fig. 2) at $\omega \to 0$, $C'' = 0$.

As the frequency is increased, C'' increases to a maximum of

$$C''_{max} = \frac{C_G^2}{2(C_S + C_G)} \tag{8}$$

at a frequency of

$$\omega_{max} = \frac{1}{R(C_S + C_G)} \tag{9}$$

and then decreases to 0 as the frequency $\omega \to \infty$.

The value of the real part of capacitance at $\omega \to 0$ is $C' = C_G$.

and the value at $\omega \to \infty$ is

$$C' = \frac{C_S C_G}{(C_S + C_G)} \tag{10}$$

It follows that the step change in capacitance is

$$\Delta C' = C_G - \frac{C_S C_G}{(C_S + C_G)}, \text{ or } \Delta C' = \frac{C_G^2}{(C_S + C_G)} \tag{11}$$

Measurement of Sublimation Rate and End of Primary Drying

The basic assumption is that the capacitance is a function of the amount of ice in the measurement vial and provides the rationale for the application of TVIS as a determinant of ice sublimation rate during primary drying. It has been demonstrated that TVIS can be used to measure the onset of primary drying, rate of ice sublimation and end of primary drying [42].

Equation 12 (and the explanation that follows) demonstrates how the magnitude of the peak in the imaginary part capacitance, during primary drying, provides an assessment of the remaining ice and thereby an opportunity to assess relative drying rates in vials as the process is scaled-up from the mini-piloting study (e.g. on an individual vial or a small cluster of vials).

$$C''_{max} = \frac{C_G^2}{2(C_S + C_G)} \tag{12}$$

The magnitude of each lumped circuit element $(C_S + C_G)$ is proportional to the cell constant for that element, i.e.

$$C_G = \varepsilon_G \varepsilon_0 \frac{A}{d} \tag{13}$$

and

$$C_S = \varepsilon_S \varepsilon_0 \frac{A}{d} \tag{14}$$

where A is the area of interface between the frozen mass and the glass adjacent to the electrode. Provided the sublimation interface is flat then as the ice is removed from the sample and the sublimation front recedes down the vial, then the interfacial area between the frozen layer and the juxtaposed glass wall (A) will decrease in proportion to the remaining ice volume. An electrical model of the drying process is given in Fig. 3, in which a dry-layer impedance is incorporated into the overall impedance of the system. In reality, the impedance of this layer can be ignored given that the time constant for charging the segment of glass in proximity to the dry layer is

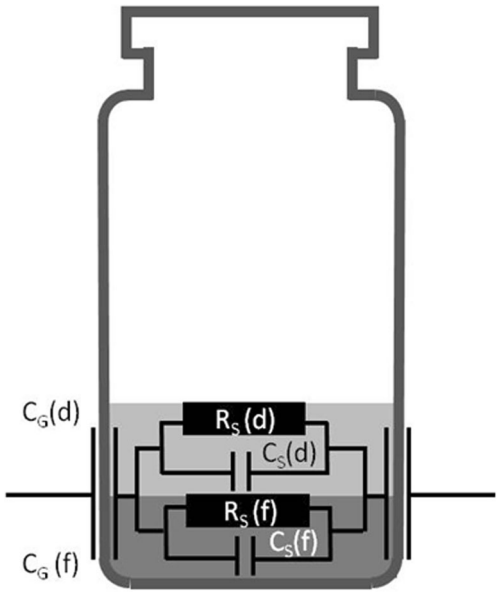

Fig. 3 Equivalent circuit model of a two-layer system, with a dry layer above an ice-rich layer. Here, the model shows an external electrode system that is of a height such that the fill volume extends both above the top and below the base of the electrode

very large, owing to the high resistance of the dried solid, and the only contribution made will be a small contribution to the real-part capacitance.

The schematic in Fig. 3 illustrates how the measured capacitance of the glass and the frozen solution will change on drying. For a linear drying rate (in time) and for a flat sublimation interface, both C_S and C_G would be expected to decrease in a linear response. However, given the fact that the electrodes do not span the full height of the liquid one then needs to consider the impact of the height of the frozen layer in relation to the electrode height on the measured response. It follows that one can expect a greater sensitivity to the frozen layer in the middle/centre region of the electrode than in the regions above and below the electrode. This feature of the measurement system in its current form (with electrodes on the outside of the vial) partly explains why one observes the sigmoidal decrease in the magnitude of the peak as the ice sublimes from the sample (Fig. 4).

To explore this observation further, one needs to consider the fill volume/height in relation to the vial size and electrode geometry being used (Although we might add that, in the classical scale-up approach in lyophilisation, one would keep the fill height the same but increase surface area in order to increase drying rates). The theoretical impact of this change in vial geometry in relation to the electrode geometry was explored in a previous publication, in which it was predicted that the relaxation frequency might increase by up to a factor of two if 2-ml vials are used instead of the 10-ml vials we have used in our work [45].

In our case, the electrode height in the current presentation of the TVIS measurement system is 5 mm, which means that for a fill volume of 3 ml, the liquid height is ~9.5 mm. The electrode is placed in such a way that it is 1–2 mm above the vial base (measured externally) and is 2–3 mm below the fill height [45]. If there is a 1–2-mm gap (i.e. ice layer) below the electrode, then there will be 2.5 to 3.5 mm of ice layer above the electrode. It follows that the response of the TVIS spectrum to a reduction in the height of the ice layer will not be registered until (2.5–3.5)/9.5 (i.e. 25% to 35%) of the ice is removed. The data generated by the TVIS system supports this observation (Fig. 5) which shows that the TVIS system only begins to register the loss of ice when the ice has reduced to approximately 20%. Thereafter, the TVIS system senses a linear decrease in the magnitude of the peak after approximately 40% of the ice has been removed.

Extrapolation of the linear portion of the C''_{peak} vs time plot, to the start of the primary drying phase, suggests that a

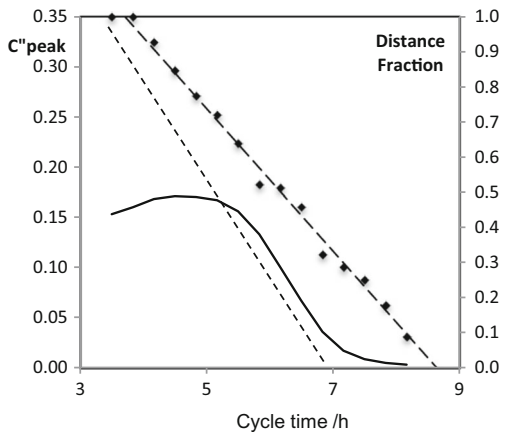

Fig. 4 Capacitance profile of 3% (*w*/*v*) lactose during primary drying; the *solid line* is C''_{peak} vs primary drying as measured by the TVIS system. The *symbols* and the *long dashed line* represent the loss of ice as determined from a visual assessment of the ice layer from the outside of the vial. The *short dotted lines* on the linear region of the C''_{peak} plot is the surrogate drying rate determined by the TVIS system

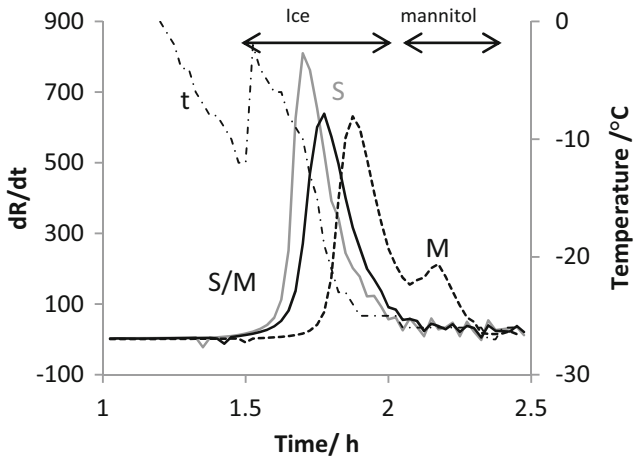

Fig. 5 The electrical resistance (d*R*/d*t*) profile during freezing of mannitol solution (*M*), sucrose (*S*) and a 50:50 mixture of mannitol and sucrose (*S/M*)

surrogate drying rate may be determined from the imaginary capacitance alone, thereby facilitating comparison between vials placed in different position in the dryer.

It remains to be seen whether any general rules may be developed which enables the drying rate of a range of formulations to be extracted from TVIS measurements. For example, what is unknown at present is the amount of ice that has formed. This uncertainty may be removed by calculating the water content of the unfrozen layer from a measurement of the glass transition temperature (see following section) and the application of the Gordon-Taylor eq. A more straightforward application of this methodology would be to use it to evaluate the heat transfer coefficient (K_v) at the base of the vial from a sublimation experiment using water (rather than the product solution). Other parameters to be recorded, in order to achieve a clear evidence of the sublimation rate, include the measurement of temperature at the vial bottom and cake resistance to vapour flow. In that case, the amount of ice is known as it is the same as the amount of water that is added to the vial [46].

Examples of the Use of TVIS in Mini-piloting (from Single to Multiple Vials) to Measure Temperature and to Characterise Critical Temperatures and Transitions

In the sections that follow a number of applications for TVIS have been described in order to demonstrate the versatility of the technique in the characterisation of first and second order phase transitions (ice formation, eutectic formation and suppression, glass transitions and phase separation), product temperature and product collapse.

In the majority of the following applications, the sensitivity of the TVIS response surface to changes in the resistance of the fill solution have been exploited to determine changes in state (e.g. liquid to solid) and the temperature of the solution (whether liquid or frozen). From Eq. 9 (re-stated here),

$$\omega_{max} = \frac{1}{R(C_S + C_G)}$$

one can see the impact of a phase change, which increases the resistance of the sample by a factor of 100–1000 whereas the capacitance will only change by a factor of 25% at best (e.g. 80 to 100). The peak frequency is therefore strongly dependent on the sample resistance.

Measurement of Eutectic Crystallisation

Classically, eutectic crystallisation of an excipient in a formulation is detected using off-line DSC studies, however, until recently there were no techniques capable of recording the manifestation of this crystallisation process in-line, and therefore, it is unclear whether there is a need to include an annealing stage in the drying cycle. The impedance measurements recorded from a surrogate formulation containing mannitol demonstrates a secondary peak in the derivative of the resistance profile at approximately −22 °C which was in close agreement with the eutectic crystallisation of mannitol as determined by DSC (Fig. 5).

During this study, the impact of a non-crystallising solid (sucrose) was also shown to suppress the crystallising behaviour of mannitol [47].

Measurement of Product Collapse

It is well known fact that the viscosity of a formulation decreases as the temperature increases above glass transition T_g'. At some temperature exceeding T_g', the viscosity of the frozen formulation is insufficient to hold its own weight and the product collapses; the corresponding temperature is called collapse temperature (T_C) [48]. The measurement of structural collapse in a product during primary drying remains a challenge for the formulation scientist. In essence, it may provide a realistic value of temperature that defines the boundary of a design space.

Conventionally, T_C is measured by freeze-drying microscopy which measures the drying front of small sample positioned at the temperature controlled freeze-drying stage under vacuum [24]. This temperature is then considered the upper temperature limit for the primary drying stage. Recently, Mujat and coworkers used an optical coherence tomography based freeze-drying microscopy (OCT FDM) to record collapse temperature of a surrogate formulation [25, 49]. The technology is advantageous as it records in-vial measurements of product collapse within a bespoke design of a single vial freeze dryer. The results from this study indicate that T_c measured by OCT FDM was ~3 °C higher than the one measured by conventional FD microscopy suggesting a higher primary

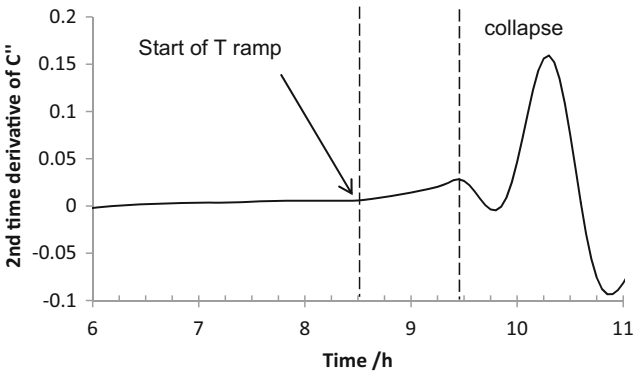

Fig. 6 Demonstration of collapse in 3% solution of sucrose as the shelf temperature is increased during the primary drying phase

drying temperature is permissible that could reduce the primary drying time by up to 30%. Although the OCT FDM system measures the response of the frozen solution within the glass vial, there are certain limitations such as: (i) only part of the formulation in direct contact with the probe is measured, (ii) the presence of the probe may perturb the ice structure and (iii) it is not possible to use the measurement system on vials placed within the usual configuration of a hexagonal array.

In a previous study [44], impedance spectroscopy has been used to record a sudden change in the capacitance (Fig. 6) which is associated with the macroscopic structural collapse of product (as measured by photographic images). This observation suggests a useful application of the TVIS in recording a failure mode.

Measurement of the Glass Transition

TVIS has been reported as a direct measurement approach which effectively measures in-vial glass transition temperatures during re-heating post-freezing (Fig. 7) [47].

The additional benefit of this approach is that the impedance data can be modelled with a modified Vogel-Tammann-Fulcher (VTF) equation which can be employed to calculate the fragility of the frozen glass. This observation refers to an additional application of TVIS for formulation screening (especially for microplate/mini-vial scale) and the potential for validation of formulation behaviour when transferred to into the process development stage (mini-piloting to scale-up). This parameter is likely to find application in determining the changes in the strength of the frozen glass following annealing which might impact the stability of the product. Such information may also provide additional information on the rationale for the inclusion of annealing step in the freeze-drying cycle [50].

Temperature Measurements

Figure 8 shows that there are correlations between log F_{peak} and product temperature during product cooling in the liquid state (A to B) and the solid state (C to D) and on annealing (D to E). The temperature coefficient for log F_{peak} in the frozen state (D to E) is ~0.04 which is approximately three times of the temperature coefficient in the solution state.

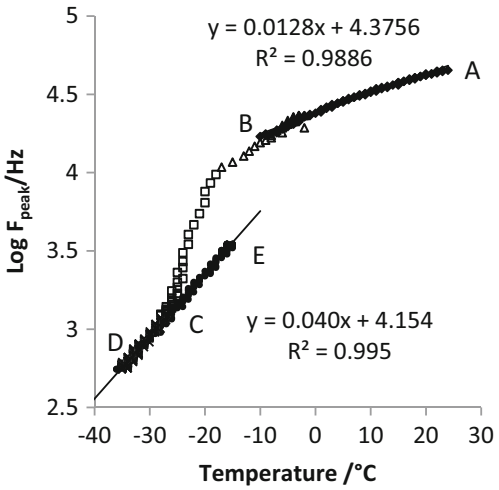

Fig. 8 Temperature calibration of the TVIS instrument, the relationship between log F_{peak} and temperature is linear, both in the liquid state (A to B) and the frozen state (C to D to E). Fitting the equivalent circulate model to the data in the region C to D to E provides an opportunity to create a model for the scenario when there may be differences in temperature between the top and bottom of the ice layer during primary drying

By fitting the equivalent circuit in Fig. 2 (ii) to the calibration model data in regions D to E, it is then possible to estimate the impact that a temperature gradient, within the vial (from the base to the top of the ice layer) will have on the spectra acquired during primary drying.

To this end, an equivalent circuit model was built comprising a number of horizontal segments (Fig. 10) with each segment comprising a parallel combination of a capacitor and a resistor. Estimates for each element were taken from the calibration data represented in Fig. 9, having taken into account the fact that the cell constants for each segment were now a

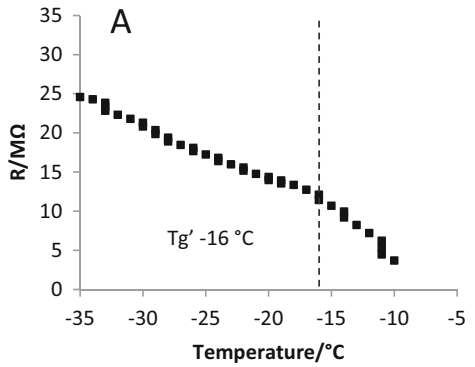

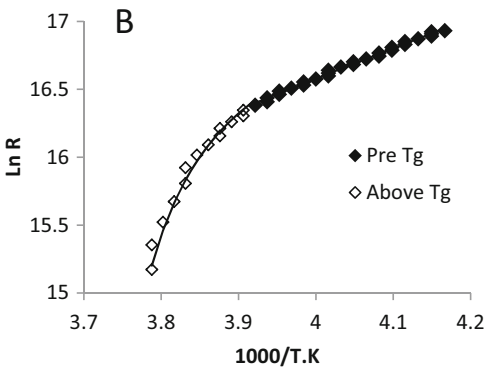

Fig. 7 Electrical impedance profile of 10% (*w*/*v*) maltodextrin DE16-19 during re-heating. **a** Temperature profile of equivalent circuit parameter *R* showing an inflexion at the glass transition temperature of −16 C; **b** Arrhenius plot of ln *R* vs 1000/*T* showing Arrhenius behaviour below T_G and non-Arrhenius behaviour above T_G (the *solid line* is the VTF model)

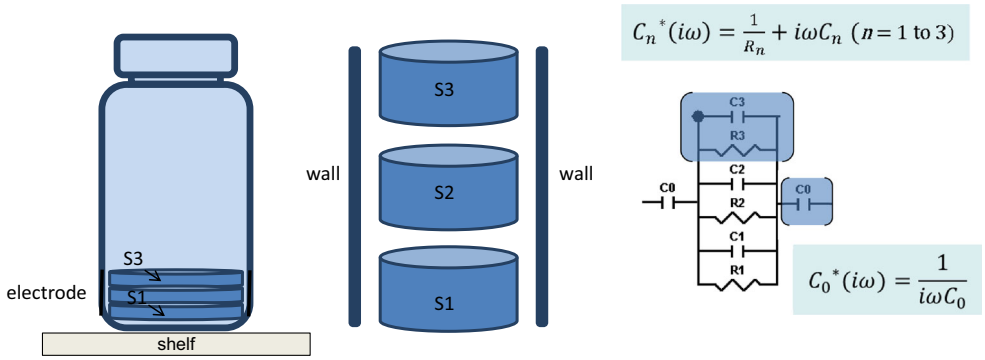

Fig. 9 Illustration of how to create a distributed circuit model to account for temperature differences between the top and bottom layers of the frozen solution. Here, three horizontal segments have been used to model a difference in temperature. In each segment, the values for the lumped circuit elements have been taken from the calibration model in the frozen state (data from regions C to E)

fraction of the cell constant for the entire volume of the sample (in the case of the capacitive element) and a multiple of the cell constant for the entire volume of the sample (in the case of the resistive element).

Results from the model (Fig. 10) suggests that the shape of the spectrum does not change when there is a distribution of temperatures across the frozen layer and that the peak frequency provides an indication of the mean temperature of the frozen mass (dashed line on Fig. 10). The mean temperature may in itself be usefully employed as the driver to set the shelf temperature in a process control scenario. In the development cycle, one might instead want to include a thermocouple in the base of the vial to measure the base temperature and then use the TVIS-derived mean temperature to predict the temperature at the sublimation interface. That would require the assumption that the profile across the frozen layer was linear.

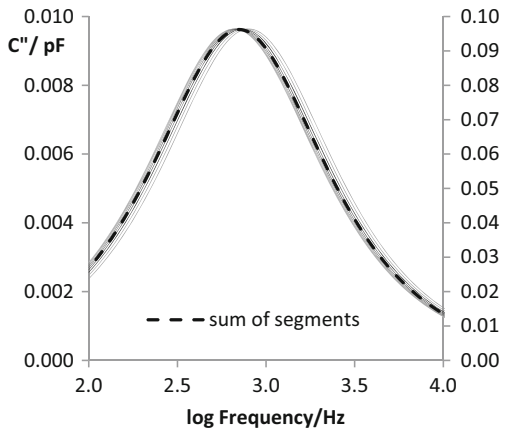

Fig. 10 Predicted response from the equivalent circuit model shown in Fig. 9 (here, the solution is divided into ten horizontal segments rather than the three shown in Fig. 9). The *left-hand scale* shows the predicted spectrum of each element, and the *right-hand scale* shows the predicted spectrum when all elements are added together. The *left scale* has been magnified by a factor to 10 so that the magnitude of the individual spectra coincides with the magnitude of the summed spectra

Characterisation of Annealing

The inclusion of annealing step increases mass transfer rates during primary drying [51] as it overcomes ice crystal heterogeneities which arise from uncontrolled freezing a stochastic process, by promoting the growth of large ice crystals which in turn reduces the dry later resistance. An annealing step is also included to promote crystallisation of bulking agent such as mannitol. TVIS has been used to improve our understanding of how drying rate changes with the annealing hold time and temperature (Fig. 11) [52].

By recording the changes in electrical impedance of the formulation during annealing as well as the primary drying stage of the freeze-drying cycle, it was possible to demonstrate that Ostwald ripening was the primary mechanism responsible for faster drying rate. Devitrification, the other mechanism in question, was ruled out as there was no significant amount of additional ice formation recorded as glass transition temperature was not increased following annealing.

The crystal growth occurs at exponential rates and this phenomenon is almost complete after 3 h. Any extension to this hold time in excess of 3 h is largely unjustified as the sublimation rate does not increase accordingly and these observations are in agreement with the R profile during annealing which records asymptote after an annealing hold time of 3 h.

Phase Separation

In certain cases, the formulation components exhibit physical incompatibility in that different phases separate out from the solution during freezing and are subsequently dried as separate layers. In order to demonstrate the potential use for through-vial impedance measurement in the determination of phase separation, a binary solution of 14% (*w*/*w*) dextran (MW 9–11,000; Sigma) and 14% (*w*/*w*) polyvinylpyrrolidone PVP K10 (Sigma) was analysed over a frequency range 100 Hz–1 MHz

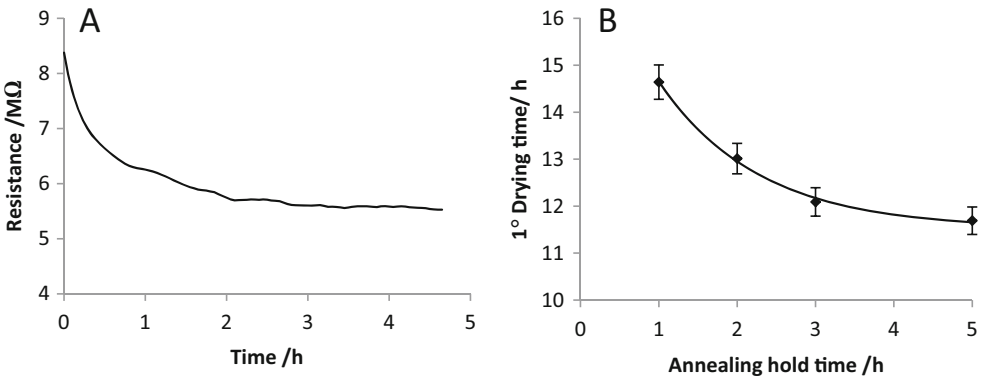

Fig. 11 **a** Resistance profile of maltodextrin 10% (*w*/*v*) during annealing hold time. **b** Impact of annealing hold time on the drying time

at scan interval of 0.5 min^{-1} throughout the following freezing cycle: temperature ramp to −35 °C in 60 min, hold then at −35 °C for 120 min and temperature ramp up from −35 to 25 °C in 60 min using a HETO FD 08 freeze dryer. The product temperature was also recorded in a neighbouring vial using a type K thermocouple. Thermal analysis of the formulation was also performed by differential scanning calorimetry, scanning over the same temperature range.

After fitting the impedance model in Eq. 1 to each spectrum, the time derivative of values of the element R_S was seen to undergo a non-linearity with temperature, which was a direct consequence of the sample passing through a glass transition. Time derivatives of the R_S parameter provided estimates for T_g' of −13 and −24 °C, whereas the T_g' estimates from DSC are −13 and −19.5 °C (Fig. 12), the latter was in agreement with T_g' of individual components reported in the literature [53, 54].

The close agreement between the two values for the T_g' of the dextran phase (at −13 °C) points to the reliability of the new method, whereas the disagreement between the two estimates for the second T_g' may point to real differences in the composition of the PVP phase.

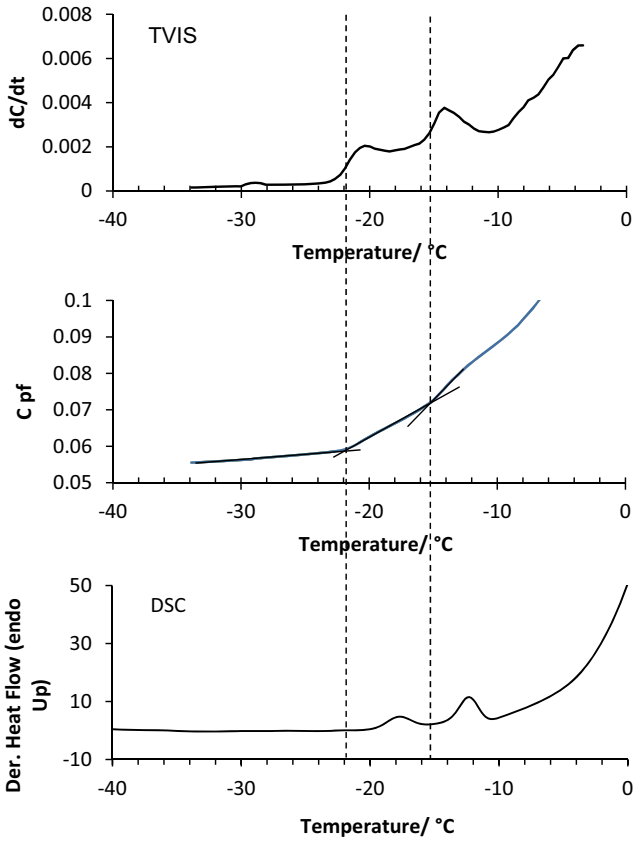

Fig. 12 **a** Time derivative and imaginary capacitance of 14% (*w*/*w*) dextran and 14% (*w*/*w*) PVP. **b** DSC scan during re-heating from −35 to 25 °C

Conclusions

We have reviewed the advantage and limitation of the various available PAT technologies, such as thermocouples, TDLAS and MTM, commonly used to monitor the freeze-drying process. The translation of process understanding from the mini-pilot to scale-up and production demands a new PAT method that can bridge these scales and provide the verification that the process parameters at one scale can be achieved at another. TVIS provides part of that solution on the basis of a two-parameter measurement: the first parameter is the measurement of the magnitude of the interfacial-relaxation process which has been shown to provide a convenient non-invasive (albeit single vial) measurement of drying rates. The second is the frequency position of the interfacial relaxation which is sensitive to both temperature and phase behaviour. The most important critical product parameter is the product temperature at the ice sublimation interface, T_p, as it defines the efficiency of the process in terms of the rate of drying. Here, we demonstrate a possible methodology for determining simultaneously the critical process parameter and the impact it has on drying rates. In future, with TVIS capability embedded in different scales or dryer, it should be possible to track the product temperature and drying rate vs. time profile so that the influence of process- and equipment-related differences may be first understood and then compensated for, and a

dynamic cycle developed which adapts the shelf inlet temperature and chamber pressure to maintain this profile. Other capabilities of the TVIS method in the determination of the glass transition and the strength/fragility of the unfrozen phase have been highlighted and suggestions provided as to the relevance these parameters have in assessment of product stability.

References

1. Tang X, Pikal M. Design of freeze-drying processes for pharmaceuticals: practical advice. Pharm Res. 2004;21(2):191–200. doi:10.1023/b:pham.0000016234.73023.75.
2. Brulls M, Rasmuson A. Heat transfer in vial lyophilization. Int J Pharm. 2002;246:1–16.
3. Guttzeit M. Designing an effective PAT-driven scale-up of lyophilization processes. PharmTechnol. 2010;22(11):8.
4. Grant Y, Dalby PA, Matejtschuk P. Use of design of experiment and microscale down strategies in formulation and cycle development for lyophilization. Am Pharm Rev. 2012;11
5. Schwegman JJ, Hardwick LM, Akers MJ. Practical formulation and process development of freeze-dried products. Pharm Dev Technol. 2005;10(2):151–73. doi:10.1081/PDT-56308.
6. Kim AI, Akers MJ, Nail SL. The physical state of mannitol after freeze-drying: effects of mannitol concentration, freezing rate, and a noncrystallizing cosolute. J Pharm Sci. 1998;87(8):931–5. doi:10.1021/js980001d.
7. Kochs M, Körber C, Heschel I, Nunner B. The influence of the freezing process on vapour transport during sublimation in vacuum-freeze-drying of macroscopic samples. Int J Heat Mass Transf. 1993;36(7):1727–38. doi:10.1016/S0017-9310(05)80159-0.
8. Rambhatla S, Tchessalov S, Pikal M. Heat and mass transfer scale-up issues during freeze-drying, III: control and characterization of dryer differences via operational qualification tests. AAPS PharmSciTech. 2006;7(2):E61–70. doi:10.1208/pt070239.
9. Konstantinidis AK, Kuu W, Otten L, Nail SL, Sever RR. Controlled nucleation in freeze-drying: effects on pore size in the dried product layer, mass transfer resistance, and primary drying rate. J Pharm Sci. 2011;100(8):3453–70. doi:10.1002/jps.22561.
10. Rasetto V, Marchisio DL, Fissore D, Barresi AA. On the use of a dual-scale model to improve understanding of a pharmaceutical freeze-drying process. J Pharm Sci. 2010;99(10):4337–50.
11. Ganguly A, Nail SL, Alexeenko A. Experimental determination of the key heat transfer mechanisms in pharmaceutical freeze-drying. J Pharm Sci. 2013;102(5):1610–25. doi:10.1002/jps.23514.
12. Patel SM, Pikal M. Process analytical technologies (PAT) in freeze-drying of parenteral products. Pharm Dev Technol. 2009;14(6):567–87. doi:10.3109/10837450903295116.
13. Barresi AA, Pisano R, Fissore D, Rasetto V, Velardi SA, Vallan A, et al. Monitoring of the primary drying of a lyophilization process in vials. Chem Eng Process. 2009;48(1):408–23.
14. Fissore D, Pisano R, Barresi AA. On the methods based on the pressure rise test for monitoring a freeze-drying process. Dry Technol. 2010;29(1):73–90. doi:10.1080/07373937.2010.482715.
15. Bosca S, Barresi AA, Fissore D. Use of a soft sensor for the fast estimation of dried cake resistance during a freeze-drying cycle. Int J Pharm. 2013;451(1–2):23–33. doi:10.1016/j.ijpharm.2013.04.046.
16. Bosca S, Barresi BA, Fissore D. Use of soft sensors to monitor a pharmaceuticals freeze-drying process in vials. Pharm Dev Technol. 2012;0(0):1–12. doi:10.3109/10837450.2012.757786.
17. Jameel F, Kessler WJ, Schneid S. Application of PAT in Real-time Monitoring and Controlling of Lyophilization Process. Quality by Design for Biopharmaceutical Drug Product Development. Springer; 2015. p. 605–47.
18. Grant Y, Matejtschuk P, Bird C, Wadhwa M, Dalby PA. Freeze drying formulation using microscale and design of experiment approaches: a case study using granulocyte colony-stimulating factor. Biotechnol Lett. 2012;34(4):641–8. doi:10.1007/s10529-011-0822-2.
19. Kauppinen A, Toiviainen M, Korhonen O, Aaltonen J, Jarvinen K, Paaso J, et al. In-line multipoint near-infrared spectroscopy for moisture content quantification during freeze-drying. Anal Chem. 2013;85(4):2377–84. doi:10.1021/ac303403p.
20. Capelle MAH, Gurny R, Arvinte T. High throughput screening of protein formulation stability: practical considerations. Eur J Pharm Biopharm. 2007;65(2):131–48. doi:10.1016/j.ejpb.2006.09.009.
21. Kauppinen A, Toiviainen M, Aaltonen J, Korhonen O, Järvinen K, Juuti M, et al. Microscale freeze-drying with Raman spectroscopy as a tool for process development. Anal Chem. 2013;85(4):2109–16. doi:10.1021/ac3027349.
22. Capelle MAH, Arvinte T. High-throughput formulation screening of therapeutic proteins. Drug Discov Today Technol. 2008;5(2–3):e71–e9. doi:10.1016/j.ddtec.2009.03.003.
23. PSI. Lyoflux: Tunable Diode Laser Absorption Spectroscopy. Physical Sciences Inc., USA. 2016. http://www.psicorp.com/case-studies/lyoflux%E2%84%A2-tunable-diode-laser-absorption-spectroscopy. Accessed 20/06/2016 2016.
24. Meister E, Gieseler H. Freeze-dry microscopy of protein/sugar mixtures: drying behavior, interpretation of collapse temperatures and a comparison to corresponding glass transition data. J Pharm Sci. 2009;98(9):3072–87. doi:10.1002/jps.21586.
25. Mujat M, Greco K, Galbally-Kinney KL, Hammer DX, Ferguson RD, Iftimia N, et al. Optical coherence tomography-based freeze-drying microscopy. Biomed Opt Express. 2012;3(1):55–63.
26. De Beer T, Burggraeve A, Fonteyne M, Saerens L, Remon JP, Vervaet C. Near infrared and Raman spectroscopy for the in-process monitoring of pharmaceutical production processes. Int J Pharm. 2010;In Press, Corrected Proof.
27. De Beer TRM, Vercruysse P, Burggraeve A, Quinten T, Ouyang J, Zhang X, et al. In-line and real-time process monitoring of a freeze drying process using Raman and NIR spectroscopy as complementary process analytical technology (PAT) tools. J Pharm Sci. 2009;98(9):3430–46. doi:10.1002/jps.21633.
28. Pikal MJ, Shah S, Roy ML, Putman R. The secondary drying stage of freeze drying: drying kinetics as a function of temperature and chamber pressure. Int J Pharm. 1990;60(3):203–7.
29. Hsu CL, Heldman DR, Taylor TA, Kramer HL. Influence of cooling rate on glass transition temperature of sucrose solutions and rice starch gel. J Food Sci. 2003;68(6):1970–5. doi:10.1111/j.1365-2621.2003.tb07003.x.
30. Pomerantsev AL, Rodionova OY. Process analytical technology: a critical view of the chemometricians. J Chemom. 2012;26(6):299–310. doi:10.1002/cem.2445.
31. Tang X, Nail S, Pikal M. Evaluation of manometric temperature measurement (MTM), a process analytical technology tool in freeze drying, part III: heat and mass transfer measurement. AAPS PharmSciTech. 2006;7(4):E105–E11. doi:10.1208/pt070497.
32. Gieseler H, Kramer T, Pikal M. Use of manometric temperature measurement (MTM) and SMART™ freeze dryer Technology for Development of an optimized freeze-drying cycle. J Pharm Sci. 2007;96(12):3402–18.
33. Tang X, Nail S, Pikal M. Evaluation of manometric temperature measurement, a process analytical technology tool for freeze-drying: part II measurement of dry-layer resistance. AAPS PharmSciTech. 2006;7(4):E77–84. doi:10.1208/pt070493.

34. Johnson RE, Oldroyd ME, Ahmed SS, Gieseler H, Lewis LM. Use of manometric temperature measurements (MTM) to characterize the freeze-drying behavior of amorphous protein formulations. J Pharm Sci. 2009;99(6):2863–73. doi:10.1002/jps.22031.
35. Gieseler H, Kessler WJ, Finson M, Davis SJ, Mulhall PA, Bons V, et al. Evaluation of tunable diode laser absorption spectroscopy for in-process water vapor mass flux measurements during freeze drying. J Pharm Sci. 2007;96(7):1776–93. doi:10.1002/jps.20827.
36. Kuu WY, Nail SL, Sacha G. Rapid determination of vial heat transfer parameters using tunable diode laser absorption spectroscopy (TDLAS) in response to step-changes in pressure set-point during freeze-drying. J Pharm Sci. 2009;98(3):1136–54.
37. Tang X, Nail SL, Pikal MJ. Freeze-drying process design by manometric temperature measurement: Design of a smart freeze-dryer. Pharm Res. 2005;22(4):685–700. doi:10.1007/s11095-005-2501-2.
38. Schneid S, Gieseler H. Evaluation of a new wireless temperature remote interrogation system (TEMPRIS) to measure product temperature during freeze drying. AAPS PharmSciTech. 2008;9(3):729–39. doi:10.1208/s12249-008-9099-8.
39. Christ M. Lyocontrol-sensor for process monitoring and for the determination of the freezing point. In: Process control and optimization. Martin Christ, Germany. 2013. Accessed October 29 2013.
40. Rey L, May JC. Freeze-drying/lyophilization of pharmaceutical and biological products. Drugs and pharamcaceutical sciences, vol 96. New York: Marcel Dekker; 1999.
41. Ward KR, Matejtschuk P. The use of microscopy, thermal analysis, and impedance measurements to establish critical formulation parameters for freeze-drying cycle development. In: Rey L, May JC, editors. Freeze drying/lyophilization of pharmaceutical and biological products. New York: Marcel Dekker; 2010. p. 112–35.
42. Smith G, Polygalov E, Arshad MS, Page T, Taylor J, Ermolina I. An impedance-based process analytical technology for monitoring the lyophilisation process. Int J Pharm. 2013;449(1–2):72–83. doi:10.1016/j.ijpharm.2013.03.060.
43. Smith G, Polygalov E, Page T, inventors; GEA Pharma Systems Limited, assignee. Electrical monitoring of a lyophilization process Great Britain patent GB2480299. 2011 16/11/2011.
44. Smith G, Arshad MS, Polygalov E, Ermolina I, Nazari K, Taylor J, et al. Through-vial impedance spectroscopy: a new in-line process analytical technology for freeze-drying. PharmTechnol. 2014;38(4):38–46.
45. Smith G, Arshad M, Polygalov E, Ermolina I. Factors affecting the use of impedance spectroscopy in the characterisation of the freezing stage of the lyophilisation process: the impact of liquid fill height in relation to electrode geometry. AAPS PharmSciTech. 2014;15(2):261–9. doi:10.1208/s12249-013-0054-y.
46. Pikal MJ, Roy ML, Shah S. Mass and heat transfer in vial freeze-drying of pharmaceuticals: role of the vial. J Pharm Sci. 1984;73(9):1224–37. doi:10.1002/jps.2600730910.
47. Arshad MS, Smith G, Polygalov E, Ermolina I. Through-vial impedance spectroscopy of critical events during the freezing stage of the lyophilization cycle: the example of the impact of sucrose on the crystallization of mannitol. Eur J Pharm Biopharm. 2014;87(3):598–05. doi:10.1016/j.ejpb.2014.05.005.
48. Sun WQ. Temperature and viscosity for structural collapse and crystallization of amorphous carbohydrate solutions. Cryo Letters. 1997;18:99–106.
49. Greco K, Mujat M, Galbally-kinney KL, Hammer DX, Ferguson RD, Iftimia N, et al. Accurate prediction of collapse temperature using optical coherence tomography-based freeze-drying microscopy. J Pharm Sci. 2013;102(6):1773–85. doi:10.1002/jps.23516.
50. Smith G, Arshad MS, Polygalov E, Ermolina I. An application for impedance spectroscopy in the characterisation of the glass transition during the lyophilization cycle: the example of a 10% *w/v* maltodextrin solution. Eur J Pharm Biopharm. 2013;85(3 Pt B):1130–40. doi:10.1016/j.ejpb.2013.08.004.
51. James A, Searles JFC, Theodore W. Randolph. Annealing to optimize the primary drying rate, reduce freezing-induced drying rate heterogeneity, and determine Tg in pharmaceutical lyophilization. J Pharm Sci. 2000;90(7):872–87.
52. Smith G, Arshad MS, Polygalov E, Ermolina I. Through-vial impedance spectroscopy of the mechanisms of annealing in the freeze-drying of maltodextrin: the impact of annealing hold time and temperature on the primary drying rate. J Pharm Sci. 2014;103(6):1799–810. doi:10.1002/jps.23982.
53. Wei W. Lyophilization and development of solid protein pharmaceuticals. Int J Pharm. 2000;203(1–2):1–60. doi:10.1016/s0378-5173(00)00423-3.
54. Izutsu K-i, Aoyagi N, Kojima S. Effect of polymer size and cosolutes on phase separation of poly(vinylpyrrolidone) (PVP) and dextran in frozen solutions. J Pharm Sci. 2005;94(4):709–17. doi:10.1002/jps.20292.